Hindawi
Advances in Civil Engineering
Volume 2021, Article ID 9997569, 10 pages
https://doi.org/10.1155/2021/9997569

Research Article

Laboratory Model Test Research on Mechanical Characteristics of Anchor in Loess Tunnel under the Action of Pull-Out Load

Zhongming Su,[1,2] Jianxun Chen ,[1] Yanbin Luo,[1] and Xin He[2]

[1]*School of Highway, Chang'an University, Xi'an 710064, China*
[2]*Key Laboratory of Highway Construction & Maintenance Technology in Loess Region, Shanxi Transportation Technology Research & Development Co., Ltd., Taiyuan 030032, China*

Correspondence should be addressed to Jianxun Chen; chenjx1969@chd.edu.cn

Received 10 March 2021; Revised 25 April 2021; Accepted 6 May 2021; Published 18 May 2021

Academic Editor: Claudio Mazzotti

The deformation mode of loess surrounding rock of anchor under the action of pull-out load and the shear stress distribution law of loess anchor and loess interface under the condition of different lengths anchor are studied by using the laboratory self-made model test chamber and micro anchor pullout instrument. A total of three tests are carried out for the selected test anchor. Three deformation modes of loess surrounding rock under the action of pull-out load are obtained according to the test results. It is proposed that the maximum shear stress of loess anchor under the action of pull-out load appears in the section 25 times the anchor diameter from the anchor head, and the shear stress in the middle and rear part of the anchor body can only be brought into full play when the length-to-diameter ratio of the anchor body is 110 or more. Based on the displacement solution of Mindlin problem, the drawn conclusion is compared with the theoretical solution of shear stress and axial force of loess anchor under the action of pull-out load. The results compared are basically consistent, indicating that the conclusion has strong engineering practice, which can provide technical basis for the design and optimization of the system anchor in the sidewall of loess tunnel.

1. Introduction

Anchoring technology, which is widely used in mine, tunnel, slope, dam foundation, and other constructions, is a crucial means of geotechnical reinforcement. Many scholars have performed considerable research on the anchoring mechanism of anchors in rock masses and loess tunnels and have obtained many significant results. System anchor is the most common support type in loess tunnel construction, and it can offer a kind of flexible support force, adjust the stress state of surrounding rock, and make good use of self-bearing capacity ultimately. During the tunnel excavation, the surrounding rock and support structure will be, to different extent, deformed due to the stress release. In rock tunnels, the system anchor is widely used, especially in good conditions of surrounding rock. Engineering practices show that the anchor has good applicability and can achieve good support effect in hard and soft rocks [1–10]. Yu and Xiong [11] studied the stress distribution law of surrounding rock with anchor support. Chen et al. [12] and Luo and Chen [13] presented an analytical method to predict the vertical load and settlement at the foot of steel ribs with the support of feet-lock pipe. Zhu et al. [14] studied the angle for setting foot reinforcement bolt based on the failure mode of shallow tunnel in loess tunnel. Chen et al. [15, 16] studied the action mechanism of feet-lock pipe and system anchor in soft surrounding rock and loess tunnel by using mathematical analysis method. Many experts and scholars have studied the stress mechanism and effect of tunnel anchor under different working conditions, and conclusions are of great significance to the scientific design and cost control of the tunnel [17–23]. Gao et al. [24] and Su and Liu [25, 26] briefly deduced the theoretical solution of axial force distribution of system anchors in loess tunnel based on Mindlin displacement and theoretical solution of plastic zone radius under the condition of elastic-plastic homogeneous soil, and the mechanical characteristics and length optimization of the system anchor in loess tunnel are analyzed, based on the

field test results, from two aspects of mechanical characteristics under pull-out load and axial force of system anchor at its neutral point in primary support. Based on the displacement solution of Mindlin problem, Li and Su [27] derived the elastic solution of shear stress distribution and axial force distribution in mortar system anchor under pull-out load and obtained the ultimate pull-out force of sidewall system anchor through the field test based on a loess tunnel on Kelan-Linxian expressway, analyzed its mechanical characteristics under pull-out load, and discussed distribution forms of shear stress and axial force in mortar anchor under different soil properties.

Many experts and scholars have done lots of researches on the mechanical characteristics of system anchor and its setting problem by means of numerical analysis, similar model test, and field measurement, which has played a positive role in promoting the understanding of its mechanical characteristics [28–32]. Lin et al. [33] conducted a direct shear test by changing the state of grouting, number of bolts, and inclination angle of the bolt to reveal the mechanical behavior of the bolt and failure mechanism of the bolted joint in the shearing process and found that, under the same normal stress, the yield displacement of the bolt decreased and the stiffness of the joint gradually increased with increased number of bolts; at the same number of bolts, their yield displacement increased with increased normal stress; grouting on the joint improved the force condition of the bolt, increased the yield displacement of the bolt, and coordinated the deformation of the grouting body and bolt; and lastly indicated that the inclination angle of the bolt has an effect on the shear strength of the joint. Lin et al. [34] proposed the modified formula for the shear strength of the bolted joint by considering the bolt influencing area as circular, defined the influence coefficient of the bolt and compared the experimental results and predicted results from the modified model verified by a direct shear test, and analyzed the influences of various factors on the shear strength of bolted joints combined with the test results.

However, there are few studies on the deformation mode of loess surrounding rock and the mechanical characteristics of system anchor by laboratory model test at present. Therefore, in order to further compare and analyze the rationality of conclusions based on the model test, a laboratory model test chamber is made to study deformation mode of loess anchor surrounding rock and shear stress distribution law of loess anchor and soil interface in cases of different anchor lengths under pull-out load. The research results can provide a reference for design and optimization of sidewall system anchor in loess tunnel and have good reference value and engineering practical significance.

2. Deformation of Loess Surrounding Rock under Pull-Out Load of System Anchor

The shear stress is zero and the displacement of surrounding rock along the direction of system anchor is also zero when there is no shear trend between system anchor and surrounding rock. The shear stress and the displacement of surrounding rock will be generated when there is a shear trend between system anchor and surrounding rock, and the displacement of surrounding rock will also increase with the increase of shear stress. When the shear stress increases to a certain value, the displacement of surrounding rock tends to be stable or the surrounding rock is destroyed. In the paper, the authors try to study the displacement mode of loess surrounding rock under pull-out load of system anchor by using the method of laboratory model test.

2.1. Production Process of the Laboratory Model Test Chamber. The laboratory model test chamber, as shown in Figure 1, is made of composite wood board with a thickness of 14 mm, with an internal clear width of 220 mm and a clear height of 170 mm. The sectional elevation of the model chamber is shown in Figure 2. There are two baffles at the front of the model chamber, with a hole in the middle of the baffle, 40 mm in diameter, to pass the test anchor conveniently. In the middle of the inner baffle, part of the wood board is cut off according to the test needs, so as to facilitate the test of the surface displacement of the loess body during the test, and a micro anchor drawing instrument is installed on the outer baffle to apply the anchor drawing load. Space between the two baffles is used to place dial indicator, resistance strain gauge data line, etc., and the test chamber behind the two baffles is used to fill the loess for the test. The model chamber is transversely reinforced with wooden strips at intervals of a certain length, as shown in Figure 3, to ensure that it is firm and reliable and can bear the load applied during the test.

2.2. Test Process. The anchor for the test is a 12 mm HRB335 threaded steel bar, and the anchorage material is epoxy AB glue. The diameter of the anchor is 20 mm. The clear distance from the anchor to the left and right sides of the model chamber is 100 mm, and the clear distance between the upper and lower sides is 75 mm, which is 3.5~5 times of the diameter of the anchor. The influence of the boundary effect of the model chamber on the test results can be ignored during the test. An angle grinder is used to polish the test anchor until the surface is smooth, and a fine abrasive cloth is used to grind the lines along the 45° direction of the anchor surface, so that the strain gauge can be bonded firmly. After that, the total resistance of strain gauge is measured by multimeter to ensure the strain gauge can work normally. Then, epoxy AB glue is used to smear the surface of the anchor body, and it is buried in the loess until it is dry and hard. The strain gauge pasted on the anchor body is connected to the static strain tester through the wires, as shown in Figure 4. The tester is grounded and connected to the computer. The strain of the test anchor is collected through the supporting software. At the same time, in order to avoid environmental factors such as temperature from affecting the strain test results, the tester is also connected to a compensation resistance strain gauge.

When filling and compacting loess in the test chamber, use red bricks and paper to secure the inner baffle wood block firmly, as in Figure 5, and lay a layer of plastic film on the side of the inner baffle close to the loess to prevent the

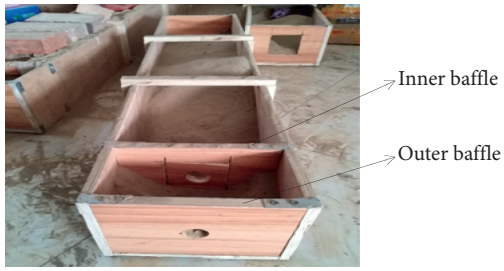

Figure 1: Laboratory model chamber for the test.

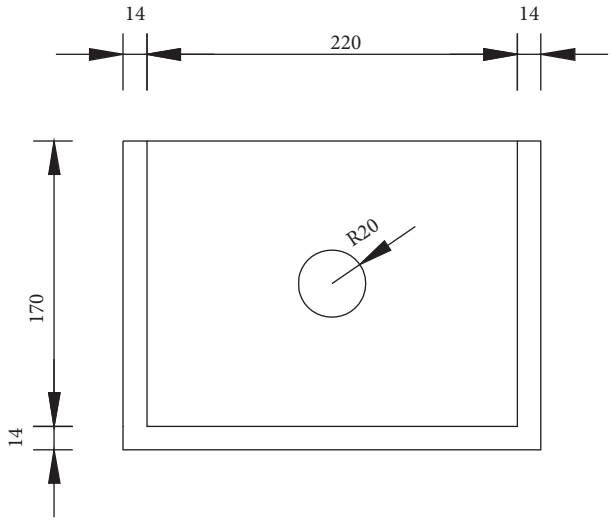

Figure 2: Sectional elevation of the laboratory model test chamber.

loess in the model chamber from flowing out during the test from the opening of the inner baffle.

In order to get closer to the stress boundary conditions in the actual anchor pull-out process, a layer of red brick is laid on the upper surface of the model chamber filled with loess, as shown in Figure 6. Install a dial indicator with an enlarged end, as shown in Figure 7, make sure its end is against the side surface of the loess body, and read the initial reading of the dial indicator. The micro anchor drawing instrument is set up at the outer baffle to prepare for applying the pull-out load. Input parameters such as strain gauge resistance and wire resistance in the static strain test software, balance the measuring points, and sample the strain value every 10 s. With the pull-out load applied by the micro anchor pulling instrument, the test officially begins. After each pressurization, the pull-out load, soil surface displacement, and anchor body strain are recorded until the three readings stabilized.

2.3. Test Principle. It is difficult to measure the internal soil deformation of the loess surrounding rock in the test. When the longitudinal depth of loess is small, the surface deformation of the soil can be used to approximately replace the internal deformation of the soil. The longitudinal depth of the loess body is 20 cm, and the anchor penetrates the 20 cm loess section to test the surface deformation of the loess surrounding rock during the anchor pull-out process. When filling the 20 cm loess section, use red bricks to support and make a hole in the center to pass the anchor body. Only fill the loess between the red brick and the inner baffle to ensure that the contact length between the anchor body and the surrounding loess is always 20 cm.

A total of 3 tests are carried out. During the test, the surface displacement of the loess surrounding rock (mm) and the pull-out force of anchor (N) are measured, respectively. Shear stress between the anchor and the loess surrounding rock, as shown in formula (1), is calculated by means of dividing pull-out force of the anchor by the contact area between the anchor and the loess surrounding rock.

$$\sigma = \frac{P}{\pi\ DL}, \tag{1}$$

where σ refers to shear stress of the test anchor, P refers to measured pull-out force of the test anchor, D refers to diameter of the test anchor, and L refers to length of the test anchor.

2.4. Analysis of Test Results. During such three tests, values of loess surface displacement measured by dial indicator and values of pull-out force measured by micro anchor pulling instrument are all listed in Tables 1~3. According to formula (1), then values of shear stress of the test anchor can be calculated, as listed in Tables 1~3. The changing trend between loess surface deformation and shear stress of the test anchor is shown in Figures 8–10, respectively.

As can be seen from Figure 11, the change trend of scatter diagram obtained in the first test can be divided into three stages: the first stage is the rigid stage, where the pull-out force increases sharply without obvious deformation of the loess surrounding rock; the second stage is the yield stage, where the pull-out force remains unchanged, and the loess surface displacement increases; the third stage is softening stage, where the pull-out force decreases and the loess surface displacement increases continuously. The deformation model of loess can be described as rigid-yielding-softening type.

As can be seen from Figure 12, the change trend of scatter diagram obtained in the second test can also be divided into three stages: the first stage is the rigid stage, where the pull-out force increases without obvious deformation of the loess surrounding rock; the second stage is the strengthening stage, where the pull-out force and the loess surface displacement increase at the same time, and the relationship between them is approximately linear; the third stage is the yield stage, where the pull-out force remains unchanged, and the loess surface displacement increases continuously. The deformation model of loess can be described as rigid-reinforced-yielding type.

As can be seen from Figure 8, the change trend of scatter diagram obtained in the third test can be divided into two stages: the first stage is the strengthening stage, where the pull-out force and loess surface displacement increase at the same time, and the relationship between them is approximately linear; the second stage is the stable stage, where the

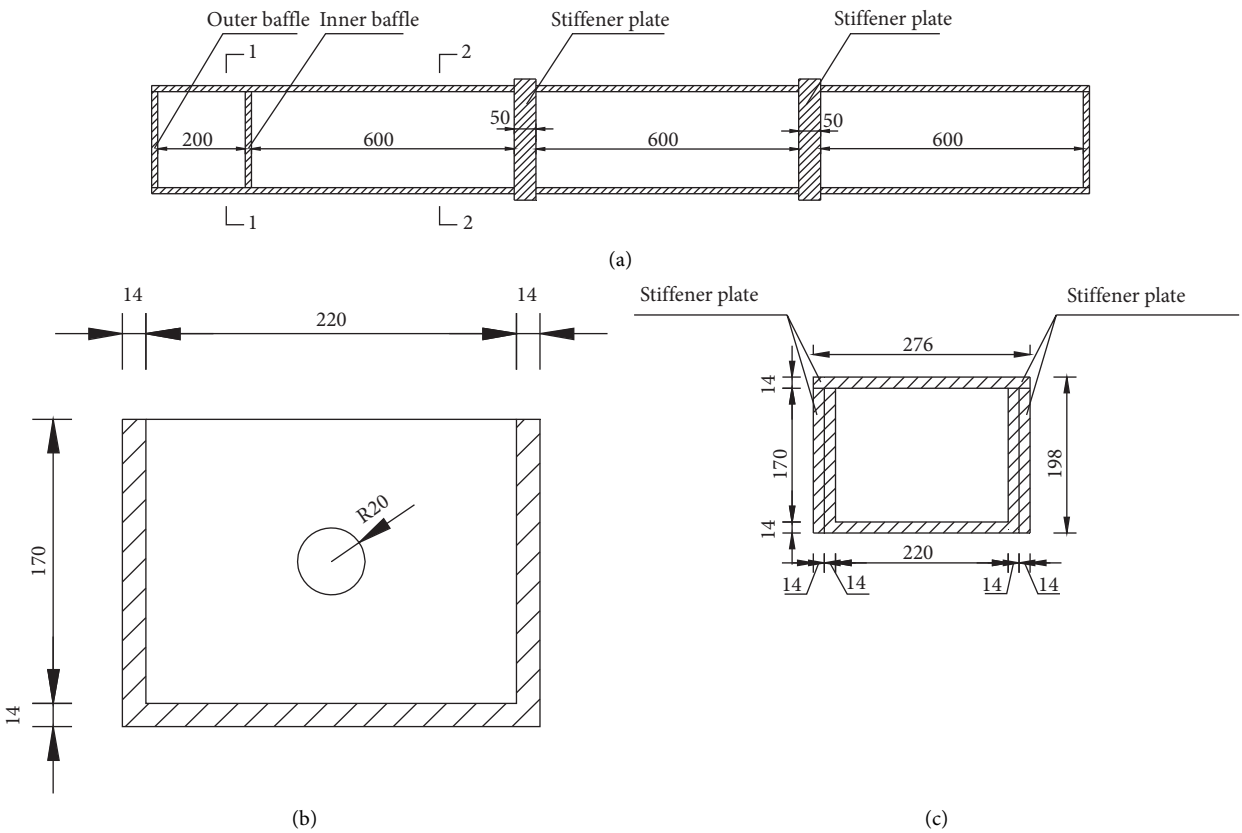

Figure 3: Plan and section of the laboratory model test chamber. (a) Plan of the laboratory model test chamber. (b) Section 1-1. (c) Section 2-2.

Figure 4: Anchors for test (HRB335, diameter = 12 mm).

Figure 5: Test anchor with pasted strain gauges (HRB335, diameter = 12 mm).

pull-out force continues to increase, and the loess surface displacement tends to stabilize. The deformation model of loess can be described as enhanced-stability type. The reason for such phenomenon above is due to the different compactness of loess filled in the model chamber.

3. Shear Stress Distribution of Interface between Anchor and Loess under Pull-Out Load

3.1. Test Cases. HRB335 threaded steel bars with a diameter of 12 mm are used in the test. The anchorage material is epoxy AB glue. The diameter of the anchoring solid is 2 cm and the spacing of strain gauges is 20 cm. The length of anchors used in the test is 40 cm, 90 cm, 140 cm, 190 cm, and 220 cm, respectively. Each type of anchor is tested three times. The 5 kinds of anchor pull-out tests all use the same loess and epoxy AB glue adhesive. The compaction of the loess and AB glue adhesive thickness are approximately equal. Therefore, the bonding strength and stiffness of the bonding surface of the 5 anchor solids and the loess are approximately equal.

The axial force of anchor can be converted from the measured strain value. The interfacial shear stress of the anchorage and the loess can be obtained by means of dividing the difference of the axial force of the adjacent strain gauges by the

Figure 6: Preparation for model test.

Figure 7: A layer of red brick laid on the upper surface of the model chamber.

Table 1: The measured test values and calculated value of shear stress (the first test).

Serial number	Values by dial indicator (mm)	Measured drawing force (N)	Calculated shear stress (kPa)
1	3.46	0	0
2	3.47	369	29.364
3	3.6	369	29.364
4	3.8	369	29.364
5	3.95	109	8.674
6	4.03	146	11.618
7	4.09	137	10.902
8	4.13	134	10.663
9	4.20	131	10.425
10	4.27	142	11.300
11	4.34	138	10.982
12	4.4	152	12.096
13	4.48	139	11.061
14	4.54	151	12.016
15	4.57	142	11.300
16	4.59	162	12.892
17	4.6	158	12.573
18	4.62	147	11.698

surface area of the anchorage in this section. The 10 cm from the end of anchor body is the test blind zone. The shear stress of this section is half of the shear stress of the 10~30 cm section and the test results are the average of three tests.

3.2. Analysis of Test Results. The shear stress distribution of the 40 cm long test anchor during the pull-out test is shown in Figure 13. It can be seen that the shear stress in the middle section of the anchor is the largest, and the shear stress in the rear section of the anchor (the longitudinal depth of loess) is larger.

The shear stress distributions of 90 cm, 140 cm, and 190 cm long test anchors during the pull-out test are shown in Figures 14–16 respectively. It can be seen that the shear stress in the front section of the anchor (near the pull-out

Table 2: The measured test values and calculated value of shear stress (the second test).

Serial number	Values by dial indicator (mm)	Measured drawing force (N)	Calculated shear stress (kPa)
1	3.17	0	0
2	3.17	115	9.151
3	3.2	158	12.573
4	3.31	149	11.857
5	3.51	230	18.303
6	3.62	209	16.632
7	3.75	207	16.473
8	3.88	196	15.597
9	3.97	210	16.711
10	4.07	200	15.915
11	4.11	188	14.961
12	4.11	177	14.085
13	4.11	227	18.064
14	4.11	220	17.507
15	4.11	217	17.268
16	4.11	213	16.950
17	4.11	210	16.711
18	4.11	205	16.313

Table 3: The measured test values and calculated value of shear stress (the third test).

Serial number	Values by dial indicator (mm)	Measured drawing force (N)	Calculated shear stress (kPa)
1	4.41	0	0
2	4.45	30	2.387
3	4.47	80	6.366
4	4.48	96	7.639
5	4.5	80	6.366
6	4.51	76	6.048
7	4.51	76	6.048
8	4.51	92	7.321
9	4.52	89	7.082
10	4.52	95	7.560
11	4.52	113	8.992
12	4.52	108	8.594
13	4.52	104	8.276
14	4.52	135	10.743
15	4.52	151	12.016
16	4.52	144	11.459
17	4.52	142	11.300
18	4.52	142	11.300

end) is the largest, and the shear stress in the middle and rear part is smaller.

The shear stress distribution of the 220 cm long test anchor during the pull-out test is shown in Figure 17. It can be seen that the shear stress of the front section of the anchor (near the pull-out end) is always the largest. As the pull-out test progresses, the shear stress of the middle and rear section also gradually increases.

Under the condition that the strength and stiffness of the bonding surface taken in the test are approximately the same, the maximum shear stress of the five types of anchor in the pull-out test appears in the section about 50 cm in front of the anchor. Among the first four types of anchor tests, the shear stress in the middle and rear part of the anchorage section is always small, and only the shear stress in the middle and rear part of the 220 cm long test anchor gradually develops and increases during the pull-out process.

Therefore, it can be inferred that the maximum shear stress of the anchor in the loess stratum under the pull-out load appears in section 25 times the diameter of the anchor away from the anchor head (position of the maximum shear stress 50 cm/diameter of the anchor 2 cm = 25). When the ratio of the anchor length and diameter is more than 110, the shear stress in the middle and rear part of the anchor body can be brought into full play (length of test anchor 220 cm/diameter of anchor 2 cm = 110).

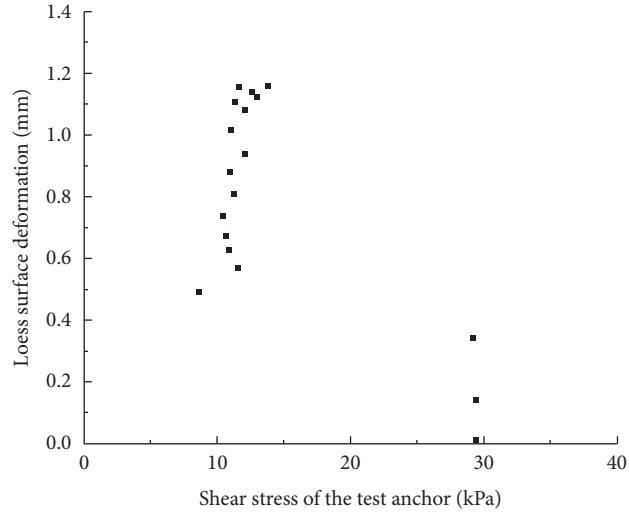

Figure 8: Changing trend between loess surface deformation and shear stress of the test anchor (the 1st).

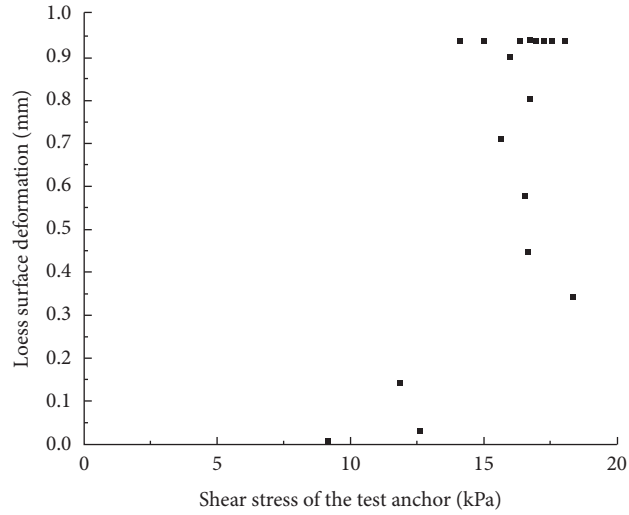

Figure 9: Changing trend between loess surface deformation and shear stress of the test anchor (the 2nd).

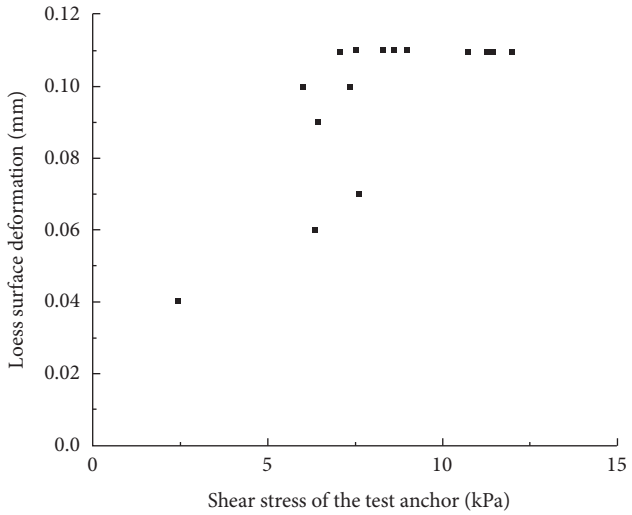

Figure 10: Changing trend between loess surface deformation and shear stress of the test anchor (the 3rd).

Figure 11: Installation of dial indicator for model test.

Figure 12: Static strain tester in work.

4. Comparison between Model Test and Theoretical Analysis

The soil acted by anchor can be regarded as a semi-infinite plane. When a concentrated force Q is applied at the depth c, the vertical displacement ω at point B (x, y, z) can be

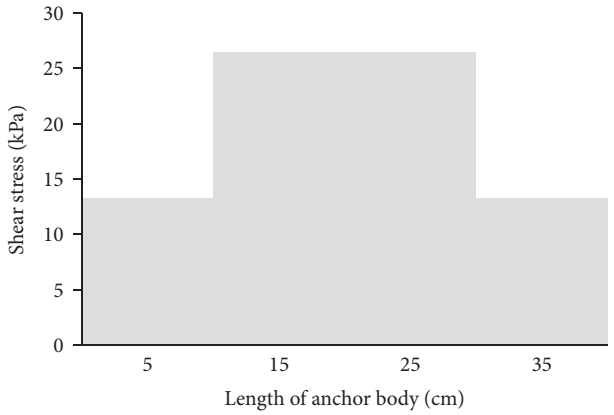

Figure 13: Shear stress distribution of anchor 40 cm.

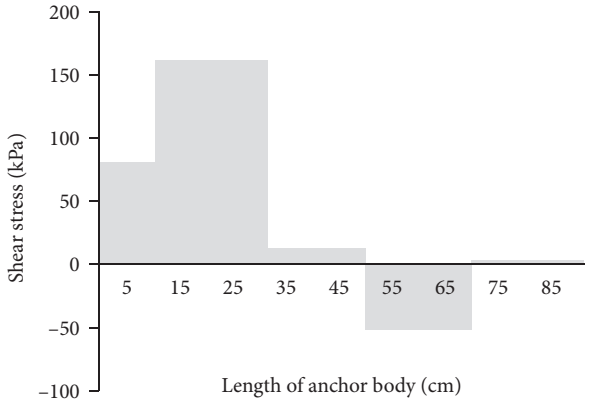

Figure 14: Shear stress distribution of anchor 90 cm.

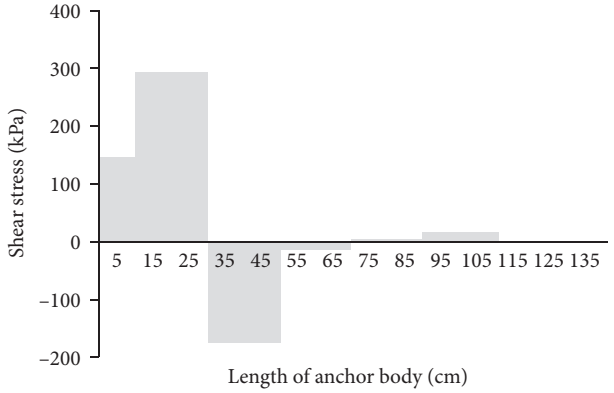

Figure 15: Shear stress distribution of anchor 140 cm.

determined by the displacement solution of the Mindlin problem. Assuming that there is no relative slip between the anchor and the deformation of loess surrounding rock, and considering the elastic deformation coordination between the proximal soil of anchor and the anchor bonding material, the analytical formula of shear stress distribution can be obtained along the anchor body in loess tunnel under the action of pull-out load by using the displacement solution of Mindlin problem. The calculation diagram is shown in Figure 18.

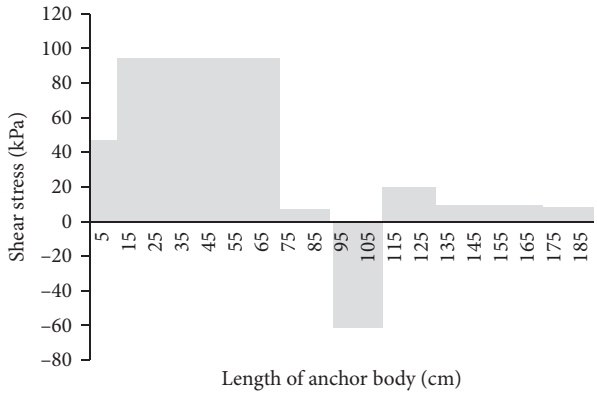

Figure 16: Shear stress distribution of anchor 190 cm.

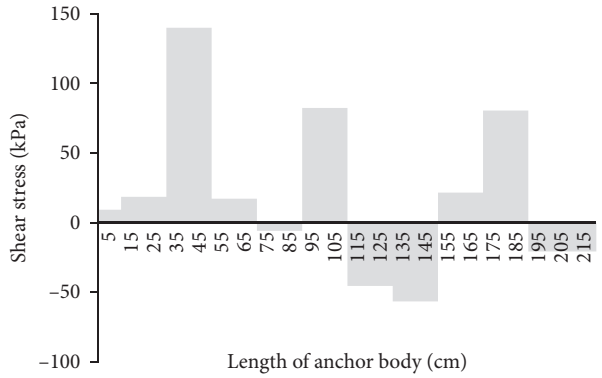

Figure 17: Shear stress distribution of anchor 220 cm.

$$\omega = \frac{Q(1+\mu)}{8\pi E(1-\mu)}\left[\frac{3-4\mu}{R_1} + \frac{(z-c)^2}{R_1^3} + \frac{8(1-\mu)^2-(3-4\mu)}{R_2} + \frac{(3-4\mu)(z+c)^2-2cz}{R_2^3} + \frac{6cz(c+h)^2}{R_2^5}\right], \tag{2}$$

where $R_1 = \sqrt{x^2+y^2+(z-c)^2}$ and $R_2 = \sqrt{x^2+y^2+(z+c)^2}$.

At the end of the anchor, $x = y = z = 0$, then formula (2) is simplified as follows:

$$\omega = \frac{Q(1+\mu)(3-2\mu)}{2\pi Ec}. \tag{3}$$

Considering the elastic deformation coordination between the proximal soil of the anchor and the anchor bonding material, the following expression is given:

$$\int_0^\infty \frac{(3-2\mu)a}{2G}\frac{\tau}{z}\mathrm{d}z = \int_0^\infty \frac{1}{E_a A}\left(Q - 2\pi a\int \tau \mathrm{d}z\right)\mathrm{d}z. \tag{4}$$

And taking into account the boundary conditions, $\tau|z_{\longrightarrow\infty} = 0$, then

$$\tau = \frac{P}{\pi a}\left(\frac{1}{2}tz\right)\exp\left(-\frac{1}{2}tz^2\right). \tag{5}$$

where $t = (1/(1+\mu)(3-2\mu)a^2)(E/E_a)$.

The analytical formula of axial force distribution along the anchor body in loess tunnel under pull-out load is as follows:

$$N = P\exp\left(-\frac{1}{2}tz^2\right), \tag{6}$$

where a is the radius of system anchor, P is the pull-out load, and E_a is the elastic modulus of system anchor.

At the same time, it is pointed out that the theoretical calculation results show that the shear stress of the anchor body reaches the maximum at the depth of 73 cm, and the attenuation rate of the axial force of the system anchor in the loess tunnel is less than its shear stress attenuation rate. The axial force of the anchor outside the 200 cm depth of the V grade surrounding rock section is already very small, which cannot achieve the desired effect. Therefore, based on the field

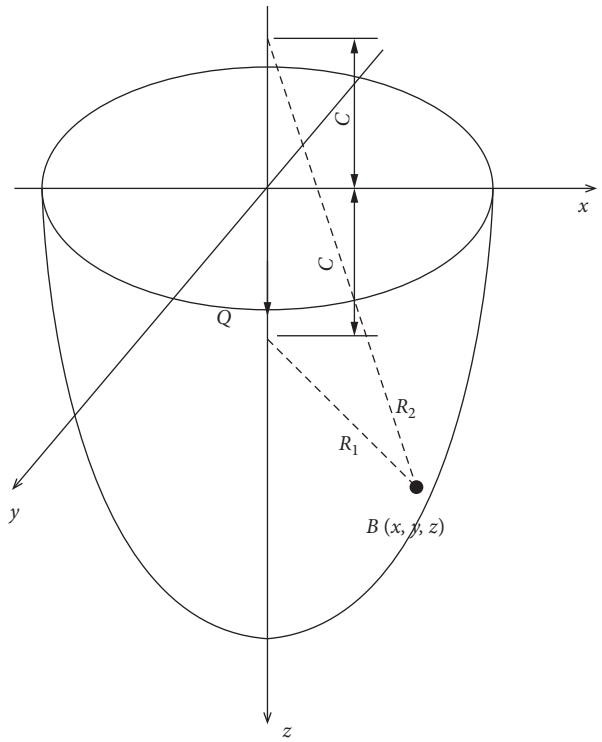

Figure 18: Calculation diagram of Mindlin displacement solution.

measured pull-out force of the anchor of loess tunnel system, the stress characteristics of the anchor can be grasped, and the design length of the anchor of loess tunnel system can be optimized on the basis of its axial force distribution. Combined with the measured axial force, the length of the anchor of loess tunnel system can be optimized to 2000 mm.

The conclusion of the model test proposed in this paper is that the maximum shear stress of the five groups of anchors in pull-out test appears in the section about 50 cm in front of the anchor body, which is basically consistent with the conclusion of the theoretical solution. When the length-to-diameter ratio of the anchor body is above 110, the shear stress in the middle and rear part of the anchor body can be brought into full play. If the HRB335 threaded steel bar with a diameter of 22 mm is used in engineering practice, the length of the anchor

(110 ∗ 22 mm = 2420 mm) can meet the needs of engineering, which is basically consistent with the conclusion of theoretical solution. Therefore, the relevant conclusions based on the laboratory model test have practical engineering reference value.

5. Conclusions

Based on the results of laboratory model test, the authors attempt to analyze the deformation mode of loess surrounding rock of anchor under the pull-out load and the shear stress distribution law of loess anchor and loess interface under the condition of different lengths anchor; the main conclusions are as follows:

(1) Under the action of pull-out load, the deformation modes of loess surrounding rock under anchor support can be summarized into three types: rigid-yielding-softening type, rigid-reinforced-yielding type, and enhanced-stability type.

(2) Under the action of pull-out load, the maximum shear stress of the anchor in the loess stratum appears in section 25 times the anchor diameter from the anchor head; only when the length-to-diameter ratio of the anchor body is 110 or more can the shear stress in the middle and rear part of the anchor body be brought into full play.

(3) The conclusions drawn from the laboratory model test are basically consistent with the conclusions based on the displacement solution of the Mindlin problem on the shear stress and axial force distribution of the loess system anchor under the action of pull-out load, indicating that the conclusion has strong engineering practice, which can provide technical basis for the design and optimization of the system anchor in the sidewall of loess tunnel.

Data Availability

The data used to support the findings of this study are available from the corresponding author upon reasonable request.

Conflicts of Interest

The authors declare that they have no conflicts of interest regarding the publication of this paper.

Acknowledgments

The authors would like to acknowledge the financial support provided by the Applied Basic Research Project of the Ministry of Transport of PRC (grant no. 2014319771190), Basic Research Project of Shanxi Province-Youth Science and Technology Research Fund (grant no.2015021121), and Science & Technology Project of Shanxi Communications Holding Group Co., Ltd. (grant no. 20-JKKJ-39). These supports are gratefully acknowledged.

References

[1] H. Duddeck, "Application of numerical analyses for tunnelling," *International Journal for Numerical and Analytical Methods in Geomechanics*, vol. 15, no. 4, pp. 223–239, 1991.

[2] J. X. Chen, Z. L. Xu, Y. B. Luo, J. K. Song, W. W. Liu, and F. F. Dong, "Application of the upper-bench CD method in super large-span and shallow tunnel: a case study of Letuan tunnel," *Advances in Civil Engineering*, vol. 2020, Article ID 8826232, 16 pages, 2020.

[3] Y. B. Luo, Z. Shi, J. X. Chen et al., "Study of deformation behaviors and mechanical properties of central diaphragm in a large-span loess tunnel by the upper bench CD method," *Advances in Civil Engineering*, vol. 2020, Article ID 8887040, 19 pages, 2020.

[4] D. Y. Li, Z. X. Xu, and L. J. Wang, "Numerical simulation analysis of the combined system of the initial support of the underground tunnel," *Railway Engineering*, vol. 34, no. 5, pp. 34–37, 2007.

[5] S. G. Zhou, L. H. Huang, S. P. Jiang, and X. R. Liu, "Study on the reasonable construction method for a loess double-arched highway tunnel," *Chinese Journal of Underground Space and Engineering*, vol. 1, no. 2, pp. 188–191, 2005.

[6] J. X. Chen, W. W. Liu, L. J. Chen et al., "Failure mechanisms and modes of tunnels in monoclinic and soft-hard interbedded rocks: a case study," *KSCE Journal of Civil Engineering*, vol. 24, no. 4, 2020.

[7] W. W. Liu, J. X. Chen, Y. B. Luo, Z. Shi, and Y. F. Wu, "Nonlinear deformation behaviors and a new approach for the classification and prediction of large deformation in tunnel construction stage: a case study," *European Journal of Environmental and Civil Engineering*, 2020.

[8] J. Qiu, Y. Lu, J. Lai, C. Guo, and K. Wang, "Failure behaviors investigation of loess metro tunnel under local-high-pressure water environment," *Engineering Failure Analysis*, vol. 115, Article ID 104631, 2020.

[9] Y. Luo, J. Chen, P. Huang, M. Tang, X. Qiao, and Q. Liu, "Deformation and mechanical model of temporary support sidewall in tunnel cutting partial section," *Tunnelling and Underground Space Technology*, vol. 61, pp. 40–49, 2017.

[10] C. Zhao, A. A. Lavasan, T. Barciaga, C. Kämper, P. Mark, and T. Schanz, "Prediction of tunnel lining forces and deformations using analytical and numerical solutions," *Tunnelling and Underground Space Technology*, vol. 64, pp. 164–176, 2017.

[11] M. Yu and F. Xiong, "Study on the law of stress distribution in the anchoring section of soil anchor," *Journal of Sichuang Water Conservancy*, vol. 27, no. 6, pp. 19–21, 2006.

[12] L. Chen, J. Chen, Y. Luo, Y. Li, and T. Hu, "Vertical load and settlement at the foot of steel rib with the support of feet-lock pipe in soft ground tunnel," *Advances in Civil Engineering*, vol. 2019, Article ID 6186748, 12 pages, 2019.

[13] Y. B. Luo and J. X. Chen, "Mechanical characteristics and mechanical calculation model of tunnel feet-lock bolt in weak surrounding rock," *Chinese Journal of Geotechnical Engineering*, vol. 35, no. 8, pp. 1519–1525, 2013.

[14] H. Y. Zhu, J. X. Chen, Y. B. Luo et al., "The angle for setting foot reinforcement bolt based on the failure mode of shallow tunnel in loess," *Tunnelling and Underground Space Technology*, vol. 108, 2021.

[15] L.-J. Chen, Y.-L. Zhang, and Z.-Y. Ma, "Analytical approach for support mechanism of feet-lock pipe combined with steel frame in weak rock tunnels," *KSCE Journal of Civil Engineering*, vol. 20, no. 7, pp. 2965–2980, 2016.

[16] J. X. Chen, J. C. Jiang, and M. S. Wang, "Function of rock bolt lattice girder and shotcrete support structure in loess tunnel," *China Journal of Highway and Transport*, vol. 20, no. 3, pp. 71–75, 2007.

[17] J. X. Chen, S. S. Yang, and Y. B. Luo, "Field test research on elimination of systematic rock bolts in weak rock tunnel," *Rock Soil Mechanics*, vol. 32, no. 1, pp. 15–20, 2011.

[18] J. Z. Wen, C. Wang, and L. B. Liu, "Research on back calculation of plastic and loose areas by axial force of rock bolt," *Chinese Journal of Underground Space and Engineering*, vol. 4, no. 6, pp. 1023–1026, 2008.

[19] X. B. Xu, T. Liu, and G. H. Chu, "Analysis on load deformation of anchoring section based on load transfer method," *Journal of Chongqing Jiaotong University: Natural Science*, vol. 29, no. 2, pp. 216–219, 2010.

[20] C. A. You, "Mechanical analysis of fully grouted anchor," *Chinese Journal of Rock Mechanics and Engineering*, vol. 19, no. 3, pp. 339–341, 2000.

[21] J. Guo, M. N. Wang, Z. S. Tan et al., "Study on the mechanical mechanism of systematic anchor in large span and shallow-buried loess tunnel," *Rock and Soil Mechanics*, vol. 31, no. 3, pp. 870–874, 2010.

[22] W.-J. Yao, W.-X. Yin, J. Chen, and Y.-Z. Qiu, "Numerical simulation of a super-long pile group under both vertical and lateral loads," *Advances in Structural Engineering*, vol. 13, no. 6, pp. 1139–1151, 2016.

[23] X. Yao, N. Li, and Y. S. Chen, "Mechanical analysis of fully grouted anchor in tunnels," *Chinese Journal of Rock Mechanics and Engineering*, vol. 24, no. 13, pp. 40–47, 2005.

[24] Y. L. Gao, D. J. Zhao, and Z. M. Su, *Loess Tunnel Engineering under Shallow Buried & unsymmetrical Pressure*, China Communications Press, Beijing, China, 2012.

[25] Z. M. Su and R. Liu, "Length parameter optimization of systematic bolt in loess tunnel based on the field test," *Applied Mechanics and Materials*, vol. 438-439, pp. 975–978, 2013.

[26] Z. M. Su and R. Liu, "Analysis of mechanical characteristic of systematic bolt in loess tunnel under the drawing load," *Advanced Materials Research*, vol. 743, pp. 86–89, 2013.

[27] Q. Li and Z. M. Su, "Analysis of difference in axial force of anchor in shallow-buried loess tunnel with large cross-section," *Applied Mechanics and Materials*, vol. 204–208, pp. 1343–1346, 2012.

[28] G. F. Chen and H. Z. Mi, "Experimental analysis of anchor's stress performance in collapsible loess layer," *Journal of Gansu University of Technology*, vol. 29, no. 1, pp. 116–119, 2003.

[29] M. F. Chen, D. G. Tang, Z. S. Zhou et al., "Test study on the anchoring mechanism of anchor," *Journal of Architectural Technology Development*, vol. 30, no. 4, pp. 21–23, 2003.

[30] Z. S. Tan, Y. Yu, M. N. Wang, and J. Yang, "Experimental study on the effect of anchor in loess deep-buried tunnel with large cross- section," *Chinese Journal of Rock Mechanics and Engineering*, vol. 27, no. 8, pp. 1618–1625, 2008.

[31] B. Q. Wang and Y. M. Men, "Test study on the model of soil anchor," *Journal of Earth Science and Environment*, vol. 31, no. 2, pp. 195–199, 2009.

[32] H. C. Zhu, R. Guan, X. Ming, and W. Tao, "Test study on the anchoring mechanism of fully grouted anchor under the drawing load," *Chinese Journal of Rock Mechanics and Engineering*, vol. 21, no. 3, pp. 379–384, 2002.

[33] H. Lin, Y. Y. Zhu, J. Y. Yang, and Z. Wen, "Anchor stress and deformation of the bolted joint under shearing," *Advances in Civil Engineering*, vol. 2020, Article ID 3696489, 10 pages, 2020.

[34] H. Lin, P. Sun, Y. Chen, Y. Zhu, X. Fan, and Y. Zhao, "Analytical and experimental analysis of the shear strength of bolted saw-tooth joints," *European Journal of Environmental and Civil Engineering*, vol. 24, pp. 1–15, 2020.